

# Frame Capture and Reliability Based Decider Implementation in the MiXiM IEEE 802.15.4 Framework

Luís M. Borges, Fernando J. Velez and  
Norberto Barroca  
Instituto de Telecomunicações, Dept. of  
Electromechanical Engineering, Universidade da  
Beira Interior  
Covilhã, Portugal  
{lborges, fjv, nbarroca}@lx.it.pt

António S. Lebres  
Department of Physics  
Universidade da Beira Interior  
Covilhã, Portugal  
lebres@ubi.pt

## ABSTRACT

The task of properly modelling the physical (PHY) layer constitutes the most challenging endeavor in wireless networks simulation. Unfortunately, today, the majority of the wireless sensor network (WSN) simulators consider a simple model for the PHY frame reception, which does not account for emerging research on the frame capture (FC) effect. In this paper, we present enhancements for the PHY layer model for the IEEE 802.15.4 standard employed in the MiXiM framework, to account for the FC effect within WSN-based simulations. These improvements are as follows: i) proposal of a formulation for the PHY layer packet reception based on a reliability concept, identified as the Enhanced Reliability Decision Algorithm, which guarantees the delivery of a packet received by the PHY layer to the medium access control (MAC) layer, with a certain value for the reliability (0.9 and 0.99); ii) different frame overlapping scenarios, and iii) different values for the thresholds to decide frame recovery. The work includes the description, implementation and performance evaluation of the proposed decision algorithm, jointly with the FC effect, in the MiXiM framework simulator, for basic MAC and scheduled channel polling (SCP) MAC protocols. Based on the simulation results, the proposed approach can significantly improve simulation accuracy and provide a PHY decision algorithm that guarantees, with a certain reliability, the delivery of frames to the MAC layer.

## Categories and Subject Descriptors

I.6.6 [Simulation of communication networks]: Simulation output Analysis; I.7 [Integration with other simulation tools]: Miscellaneous

## General Terms

Design, Simulations

Permission to make digital or hard copies of all or part of this work for personal or classroom use is granted without fee provided that copies are not made or distributed for profit or commercial advantage and that copies bear this notice and the full citation on the first page. To copy otherwise, to republish, to post on servers or to redistribute to lists, requires prior specific permission and/or a fee.  
Simutools 2014, March 17-19, Lisbon, Portugal  
Copyright © 2014 ICST 978-1-63190-007-5  
DOI 10.4108/icst.simutools.2014.254639

## Keywords

Frame Capture Effect, Packet Recovery, MiXiM, Physical Layer

## 1. INTRODUCTION

The frame capture (FC) effect occurs at the physical (PHY) layer, under some conditions, when two (or more) signal transmissions spatially and temporally overlap at a receiver. The simultaneous detection of two frames at a receiver is generally regarded as a collision. Although this is theoretically true, in the last years, the work from some researchers [12, 4] has shown that this assumption is not absolutely true. Under certain channel conditions and circumstances, the FC effect occurs when the strongest signal causes the other signals to be treated as noise (or interference) whilst being filtered out by the receiver. As a consequence, a packet is received even though a collision has occurred due to concurrent transmissions [12]. This effect neglects the assumption of “*collision as failure*” in which packet collisions leads to packets corruption. This assumption is commonly accepted in simulations [17] and research on collision avoidance schemes [13]. To the best of our knowledge, even though the FC effect has been mentioned and observed in a wide variety of radio transceivers, including IEEE 802.11, Bluetooth radio and cellular systems, in the literature, the availability of simulators that support this effect for the IEEE 802.15.4 standard is scarce. In this work the objectives are twofold: implement and integrate the FC effect in the MiXiM framework for an IEEE 802.15.4 PHY layer jointly with a new PHY layer packet reception formulation. The formulation is based on a reliability concept, identified as the Enhanced Reliability Decision algorithm which accounts the signal-to-noise-plus-interference ratio (SNIR) and the size of the packet with a certain reliability,  $\delta = \{0.9; 0.99\}$ .

The remainder of this paper is organized as follows. Section 2 addresses the related work for the impact of FC on the performance of common networking protocols that comply with IEEE 802.11 and 802.15.4 standards. Section 3 describes the FC effect concept, namely the work principles, main causes and overlapping regions to be considered in the implementation. Additionally, a brief discussion about current wireless networks simulators with the FC effect is carried out. Section 4 describes the implementation of the FC effect as well as the Enhanced Reliability Decision algorithm

in the MiXiM framework. Section 5 defines a simulation scenario for wireless sensor networks (WSNs) with the FC effect feature. Section 5 also addresses simulations that have been carried out to show the impact on the performance and gains between the proposed Enhanced Reliability Decision algorithm (for different values of reliability) with FC and the default decider algorithm, for a simple medium access control (MAC) and scheduled channel polling (SCP) MAC [18] protocols for the probability of success and throughput metrics using the MiXiM framework. Finally, Section 6 gathers the main contributions and results from the paper and presents suggestions for further research.

## 2. RELATED WORK

To the best of our knowledge, even though the frame capture effect has been mentioned and observed in a wide variety of radio transceivers, in the literature, the availability of simulators that support this effect and are compliant with the IEEE 802.15.4 standard is scarce. Several works have addressed the impact of FC on the performance of common networking protocols. The authors from [3] refer to FC as PHY layer capture, and conclude that this effect is larger at lower bit rates, by means of simulations in QualNet (to support their conclusions). The authors from [11] performed the most complete real-world experiments, investigating the behaviour of FC in detail, while adding more information to the FC notion. These authors have discovered that, apart from the SNIR, the arrival time of the frames is also important, i.e., to decide whether a frame can be captured or not. They have introduced the notion of different regions, where the overlapping of frames can occur. Even though this work has been entirely developed for the IEEE 802.11a standard, it can be considered as a solid basis to extract useful insights to guide the implementation of the FC in an IEEE 802.15.4 compliant PHY layer. In [4], the authors have sought to determine the best way to use multiple receivers in a single-hop network cluster whilst comparing the advantages of receivers on multiple channels, with the enhancement in the capture effect when multiple receivers are on the same channel. The work on IEEE 802.11a from [11] is considered by the authors [4] while considering the Shuffle link-layer protocol, which enables to reorder and schedule packet transmissions to take advantage of the message-in-message (MIM) capabilities of some wireless cards.

## 3. FRAME CAPTURE EFFECT

This section describes in detail the frame capture concept. The principles of the FC concept, as well as the main reasons for it to occur are presented and described. The different frame overlapping regions considered for the proposed integration in MiXiM framework are also described. Additionally, an outline of the state-of-the-art in terms of implementation of the FC effect in the WSN simulators is also given.

### 3.1 Work Principles

It is worthwhile to understand how the frame capture deals with two (or more) interfering signals at the hardware level. There is not a clear explanation on how the interfering signals are handled at the PHY layer with FC implemented. Therefore, a clear description of the FC behaviour is in order, as it gives insights on how to implement the FC effect

in a simulation framework. Frame capture can occur in different overlapping regions. Many variables may influence the receiver behaviour and therefore the possible occurrence of a collision. Besides, there are thresholds involved in the decisions for accepting frames when FC is enabled.

If two or more frames are being transmitted “simultaneously” or are overlapping each other, the following factors should be taken into account:

- **Received signal strength indicator (RSSI)** - One of the two signals has to be sufficiently stronger than the other one in order the receiver to be able to decode it, even if a weaker interfering signal is present;
- **Frame time arrival** - The time interval between two (or more) interfering frames is very important. Depending on the time of arrival (ToA) of the interfering signal and the beginning of the overlapping region, this will correspond to different sections of the frame;
- **Chipset manufacturer** - Depending on the frame time arrival and the chipset manufacturer, different conditions should be met in order the FC to work. The CC2420 [2, 5] can capture the stronger frame even after the reception of the weaker frame’s preamble (i.e., there is independence between the ToA of the frames).

In this work, we consider a network composed by nodes that move randomly and operate with different MAC protocols. Therefore, we intend to study the worst case scenarios, when nodes transmit overlapping packets. In such regions, the characteristics of FC effect in IEEE 802.15.4 is going to be investigated and implemented in the MiXiM [15] simulation framework which considers an offset quadrature phase-shift keying (OQPSK) modulation format with direct-sequence spread spectrum (DSSS).

### 3.2 Main Causes

In the context of the MAC protocols in the absence of an RTS/CTS scheme (broadcast traffic is considered), nodes are less aware of the surrounding traffic as well as of the transmissions of their neighbouring nodes. This leads to possible hidden terminals among nodes. Other MAC protocols, such as the SCP-MAC [18], do not consider the traditional CSMA/CA avoidance mechanism. Rather, they consider a double contention window mechanism with a preamble between both contention windows, which is sent by the nodes that won the first contention window. Two types of collision may occur. First, preamble collisions occur when nodes choose the same time slot in the first contention window, to simultaneously perform carrier sense (CS) and initiate the transmission of the preamble. Second, data packet collisions occur when the nodes that won the first contention window gain access to the second contention window and start simultaneously transmitting the data packet in the second contention window. In this protocol, the data is only lost when data packet collisions occur. The occurrence of a preamble collision does not mean an effective data packet loss.

### 3.3 Frame Capture Regions

Based in the literature [11, 3, 5] and the experience acquired during the implementation of the FC effect in the MiXiM framework simulator [4, 11], two sets of interference regions can be defined. The former considers the relevant

scenarios in which a maximum of two frames (the interfering and the desired ones) reach almost simultaneously the receiver. The latter addresses the cases with more than one interfering frame overlapping the desired signal whilst considering the same regions. One assumes that the strongest frame is always the desired one, since the content of the frames cannot be used to distinguish them. Receiving the strongest frame is a good decision in these cases because a strong SNIR corresponds to a low bit error rate (BER) which, in turn, leads to a higher conditional frame capture probability (CFCP). Hence, it is reasonable to assume that the objective of a node with the FC feature enabled is to receive always the strongest frame.

The authors from [5] present an extension of the work from [17] where they continue the initial work of the characterization of the FC effect with the CC1100 transceiver whilst expanding the analysis in order to include a general model to predict FC gains. Since in our work we intend to consider the CC2420 radio transceiver, for the sake of simplicity, only three main sections are considered: i) a preamble, ii) a sync word, and iii) a data field. Depending on the section of the frame that suffers collision, the packet success rate (PSR) differs. Considering this packet format there are five possible collision scenarios. Due to the lack of space we only present a diagram for the FC regions with more than one interfering frame. Nonetheless, the scenarios with one interfering frame are included in the abovementioned diagram, as shown in Figure 1.

The authors from [11] show the different FC regions with different timing and signal SIR situations for the Atheros chipsets. In their work the following assumption is considered: The receiver “locks” onto a frame if it has received the respective preamble and it is currently in the phase of demodulation and reception of that frame. From this point forward, the receiver considers all the remaining frames in the medium as noise and ignores the interference.

Even though the work from [11] is targeted to the IEEE 802.11a, insights can be extracted. The values of signal to interference ratio (SIR) proposed for the IEEE 802.11a with the FC feature are considered for the FC feature implementation in the MiXiM framework as a starting point, whilst considering an IEEE 802.15.4 compliant PHY layer.

In the classification of the overlapping regions [11], a distinction is made between the nodes. The sender is the node transmitting the desired frame while the other nodes are named interferers.

In the work from [4], the authors made experiments for the same overlapping regions with the CC1100 radio transceiver, which is similar to the one used in our simulations (i.e., CC2420). However, the former one is not IEEE 802.15.4 compliant and has a maximum bit rate lower than one from CC2420. Moreover, the modulation schemes are different for each one of the radios. Hence, even though the radio transceivers are not the same, the insights that can be extracted have also been considered to implement the FC feature in the MiXiM framework, considering the CC2420 radio transceiver.

In Figure 1 interfering packets that are numbered from 1 to  $k$  are simultaneously transmitted. This way, the PHY layer presents a more robust behaviour if a higher number of interfering packets are transmitted.

The time intervals  $\varphi_1$ ,  $\varphi_2$  and  $\varphi_3$  presented in Figure 1 are given in seconds and are defined as  $\varphi_1=\varphi_3=0.01$  s and

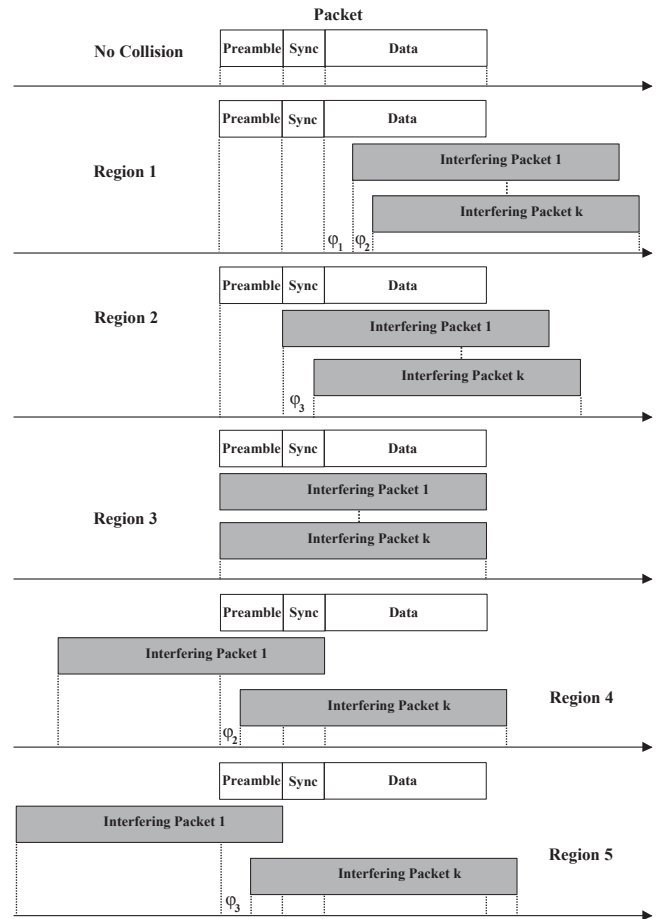


**Figure 1: Frame capture regions with more than one interfering frame.**

$\varphi_2=0.001$  s. Table 1 presents the ToA (time instant when the receivers initiates the reception of the packet). Since with more than one interferer regions 4 and 5 are different in the sense how the interfering signals overlap the desired packet, the notion of time of ending (ToE) has to be introduced and is also presented in Table 1. The ToE is defined as the time instant when a packet ends. For regions 1, 2 and 3 the first packet to arrive at the receiver is the desired one, while in regions 4 and 5 the desired signal arrives after the interfering signal. For all the regions is assumed the time instant when the desired signal is transmitted as a time reference to initiate the transmission of the interfering signals. Table 1 presents the ToA and ToE time instants of the desired and interfering frames that we consider to induce the different overlapping regions in the simulator.

From the analysis of these overlapping sections the receiver signal falls into one of the following three cases: the receiver i) receives the first received signal, ii) discards the first signal and receives the second signal, or iii) discards all packets due to excessive interference.

### 3.4 Frame Capture Effect in Simulators

The FC effect behaviour has been fairly documented for IEEE 802.11a and IEEE 802.11p wireless communication systems. However, it is not a common feature in many wireless network simulators yet, namely WSN simulators. There

**Table 1: ToA and ToE time instants of the interfering signals.**

| Collision Region | 1 <sup>st</sup> interfering packet               | 2 <sup>nd</sup> or $k^{th}$ interfering packet               |
|------------------|--|--|
| 1                | $ToA_{1a} = t_{preamble} + t_{sync} + \varphi_1$ | $ToA_{1b} = t_{preamble} + t_{sync} + \varphi_1 + \varphi_2$ |
| 2                | $ToA_{2a} = t_{preamble} + \varphi_1$            | $ToA_{2b} = t_{preamble} + \varphi_1 + \varphi_3$            |
| 3                | $ToA_{3a} = ToA_{packet}$                        | $ToA_{3b} = ToA_{packet}$                                    |
| 4                | $ToE_4 = t_{preamble} + t_{sync}$                | $ToA_4 = \varphi_2$  |
| 5                | $ToE_5 = t_{preamble}$                           | $ToA_5 = \varphi_3$  |

are some simulators that try and simulate this effect, such as the ones for infrastructured networks (not for mobile or ad-hoc ones), or it is implemented in a way that does not reflect all possible scenarios identified by the authors from [11]. In the current work, the intention is to implement the various scenarios presented in Figure 1 (i.e., with the presence of one or  $k$  interfering frames). QualNet, ns-2 [8], yet another network simulator (YANS) [10] and ns-3 [14] have the FC feature implemented on them. However, the latter is intended only for the IEEE 802.11 standard, while the former one is only available commercially. In light of these facts, there is a lack of availability of simulators dedicated to WSNs with the FC feature implemented in them. The majority of the simulators does not include this feature or it only covers some frame capture effect scenarios. Most of the simulators present fairly accurate methods for BER computation, although they only consider additive white Gaussian noise (AWGN) channels. Moreover, unlike some mentioned simulators, the MiXiM framework allows for choosing a different channel model (besides the AWGN model), such as the Rayleigh channel model. Since OMNeT++ is the elected simulator in our research group and there is no FC feature available in it, this work also aims at extending the MiXiM framework [9] in order to support the FC feature with the modulation schemes of the IEEE 802.15.4 standard.

## 4. IMPLEMENTATION OF THE FRAME CAPTURE EFFECT IN MIXIM

In this section we introduce an overview of the PHY layer as well as the description of behaviour from the default *Decider* and the new Enhanced Reliability Decision algorithm implemented in the MiXiM framework. In addition, details concerning the implementation of the FC effect in the MiXiM framework along with the FC decision thresholds are also given.

### 4.1 Physical Layer and Decision on Frames

The main objective of the PHY layer in MiXiM is to send and receive frames, applying the channel effects, by modelling, collision detection and bit error computation. The following description applies to the current, unmodified implementation of MiXiM PHY layer [9], without any modifications required to support the FC.

Different modules make part of the PHY layer of the MiXiM framework, as described in the work from [9]. However, the one that is responsible for the acceptance or rejection of frames is the *Decider*, as depicted in Figure 2.

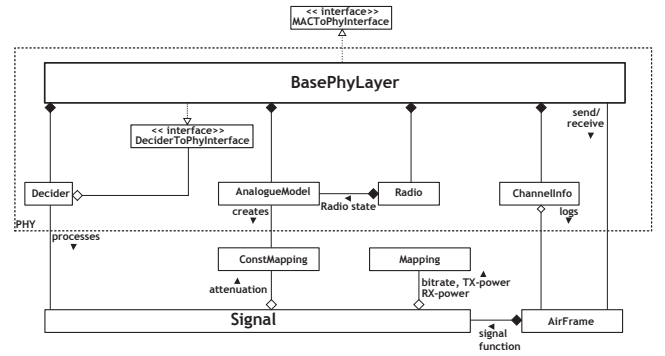


**Figure 2: MiXiM PHY layer diagram (extracted from [16], Figure 2).**

The *Decider* is the module responsible for evaluating whether the *AirFrame* (i.e., is the notation given in MiXiM framework to a frame) is received or not. In Figure 2, the *Decider* evaluates the received *Signals* whilst calculating the BER, which includes the distinction between the ones that are assumed as interference and the ones that are assumed as the desired signal.

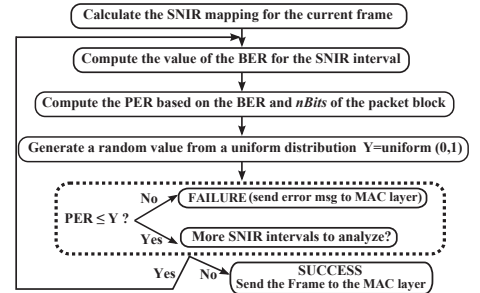


**Figure 3: Flow diagram for the default *Decider* of the MiXiM PHY layer.**

For more details regarding the SNIR mapping procedure and other tasks for the IEEE 802.15.4 PHY layer of MiXiM consult reference [9]. In Figure 3 is shown the default *Decider* procedures employed by PHY layer of MiXiM. The receiver node decides if the packet is received or not as follows:

The receiver gets the list of all *AirFrames* that were added to the *ChannelInfo* object, in order to compute all the required mappings for the SNIR computation; Depending on the overlapping of frames, different intervals can be identified as well as the mappings associated to each of the intervals. Suppose that the receiver identifies five intervals when it gets the list of all *AirFrames*; The receiver iterates all the five intervals and calculates the corresponding value for the BER for each interval and the given RSSI, noise and SNIR mappings; The receiver verifies all the different SNIR intervals of the packet and calculates the values of PER based on the BER values. As the algorithm moves from one iteration to another, if there is a higher PER value than the randomly generated variable then the packet is immediately discarded. Otherwise, is accepted.

Coding and error correction codes are not implemented in the simulator yet. Therefore, the method for BER calculation from the current *Decider* is maintained. In the default *Decider* implementation, the computation of the BER is based on the IEEE 802.15.4 PHY layer [1]. The 2.4 GHz PHY specified for this standard uses a quasi-orthogonal modulation scheme, where each symbol is represented by one of 16 nearly orthogonal PN sequences (OQPSK-16). This is a power-efficient modulation method that achieves low signal-to-noise ratio (SNR) and signal-to-interference Ratio (SIR). The BER is calculated by Equation 1, as follows:

$$BER = \frac{8}{15} \times \frac{1}{16} \times \sum_{k=2}^{16} -1^k \binom{16}{k} e^{(20 \times SNIR \times (\frac{1}{k} - 1))} \quad (1)$$

Equation 2 presents the packet success rate (PSR), which is the probability that the frame has no errors, while  $nBits$  is the length of the frame (in bits).

$$PSR = (1 - BER)^{(nBits-1)} \quad (2)$$

Equation 3, allows for computing the packet error rate (PER) for the entire packet:

$$PER = (1 - PSR) \quad (3)$$

However, the way how the *Decider* evaluates if the section of the packet is received with success (or not) needs to be updated. The values of the PER against the uniformly distributed random variable (from the default *Decider*) does not meet the FC requirements and acts as a “blind” decider agent. The *Decider* does not takes into account if the conditions of the channel are the same or not. As so, a modification is needed aiming at meting the FC requirements.

## 4.2 Enhanced Reliability Decision algorithm

The default *Decider* implementation employs an algorithm, that enables to decide if the frame is correctly decoded or not. This algorithm performs the final decision of accepting the packet or not, based on the comparison of a number randomly generated with the value obtained for PER. Some simulations have been performed considering the default *Decider* for the collision (frame capture) scenarios shown in Figure 1 (but considering a single interfering frame) and allowed for extracting the number of packets received with success and the discarded packets along with the corresponding values of the BER and PER. After plotting the PER as a function of the SNIR for the successful and discarded packets, we concluded that, for the same PER (same BER and packet length) the packet may be either received with success or discarded. This occurs because the default *Decider* acts like a “blind” decision algorithm that does not take into account if the conditions are the same, i.e., equal value of BER and packet length may cause the packet to be discarded sometimes and other times to be accepted. Therefore, maintaining the default *Decider* jointly with the implementation of the FC effect would lead to unexpected results or even worse results than with no FC feature implemented.

To sort this issue out the Enhanced Reliability Decision algorithm is added to the implementation of the *Decider*, even when the FC is not enabled.

The concept of reliability is defined for some applications as the data integrity and the level of guarantee of all the in-

formation sent by the transmitter that is accurately received at the receiver [6]. The PHY layer in a digital communication system has to ensure that the transmitted bits are reliably reconstructed at a target receiver. The reliability at the PHY layer is characterized by metrics like the SNIR, BER, symbol error rate (SER), PER, and outage probability. Achievable delivery of packets for reliable communications that rely on the values of the BER for IEEE 802.15.4 may simply be used considering the alternating bit protocol over a binary symmetric channel (BSC) channel. This reliability guarantees a dependency between the desired reliability and the values of the BER for a certain packet length [7]. Based on the Equations 2 and 3 for PSR and PER, the number of trials,  $i$ , needed to successfully transmit the packet over the link can be approximated to a geometric random variable  $X$  with the following probability mass function:

$$Pr[X = i] = PSR(nBits) \cdot PER(nBits)^{(i-nBits)}, i \in \mathbb{N} \quad (4)$$

and the following cumulative distribution function [7]:

$$F(k) = Pr[X \leq i] = \sum_{i=1}^k Pr[X = i] = 1 - PER(nBits)^k \quad (5)$$

where  $k \in \mathbb{N}$ . If the aim is to guarantee a certain delivery probability  $\delta \in [0; 1]$ , the PHY layer may define the minimum number of trials,  $k^*$ , to successfully send the packet to the receiver with a probability whose value is at least  $\delta$  (N.B.  $\delta$  is the reliability). The value of  $k^*$  is also directly proportional to the energy consumption, and is given by:

$$k^* = F^{-1}(\delta) = \min\{k \in \mathbb{N} : F(k) \leq \delta\} \quad (6)$$

Conceptually,  $k^*$  is the  $\delta$ -quantile of the random variable  $X$ . After some manipulation, one obtains:

$$k^* = \left\lceil \frac{\log(1 - \delta)}{\log(PER(nBits))} \right\rceil \quad (7)$$

where the  $\lceil \cdot \rceil$  represents the ceiling function. The number of trials,  $k^*$ , is represented in Figure 4 as a function of the BER for packets lengths  $nBits = 64$  and 336 bits. Two different values are considered for the reliability ( $\delta$ ),  $\delta_1 = 0.9$  and  $\delta_2 = 0.99$ . The plot presented in Figure 4 does not consider the ceiling function from Equation 7.

Figure 4 shows that for relaxed reliability requirements (i.e.,  $\delta_1 = 0.9$ ) and moderate-to-high bit error rates, in the range  $[10^{-5}, 10^{-4}]$ , the system wastes significantly less energy than for a more demanding reliability with  $\delta_2 = 0.99$ . With  $\delta_1 = 0.9$  the number of trials  $k^*$  needed to correctly deliver a packet is higher for higher packet lengths, as the value of the BER increases. If the value of the reliability is augmented ( $\delta_2 = 0.99$ ) the number of trials needed to correctly deliver a packet is always higher than for  $\delta_1 = 0.9$ , with packet lengths of 64 and 336 bits, as shown in Figure 4. Below a BER of approximately  $10^{-4}$ , for the considered packet lengths, the channel quality is already appropriate enough to successfully transmit the packet at the first trial while guaranteeing the target reliability bounds. Therefore, we define that  $k^* \leq k_{max}^*$ , where  $k_{max}^*=1$  is the maximum number of trials to ensure that the packet is delivered with a certain reliability,  $\delta$ . The proposed reliability concept [7] is included

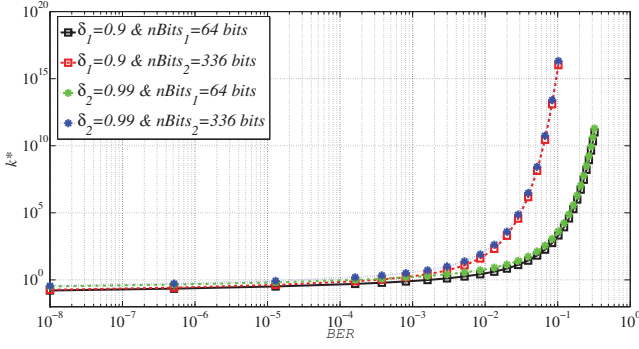


Figure 4: Minimum number of trials,  $k^*$ , as a function of the BER for  $\delta \in \{0.9; 0.99\}$  and  $nBits \in \{64; 336\}$  bits.

in the new implementation of the *Decider* in order to make a proper decision algorithm, which establishes whether the packet is received with success or not. The algorithm is implemented in MiXiM and we considered the two above-mentioned values for the reliability,  $\delta_1 = 0.9$  and  $\delta_2 = 0.99$ . However, other reliability values can be considered. The algorithm utilizes the Equation 7 to decide if the packet is received with success, which occurs if the condition  $k^* \leq 1$  is verified. Otherwise, if  $k^* > 1$ , the packet is discarded.

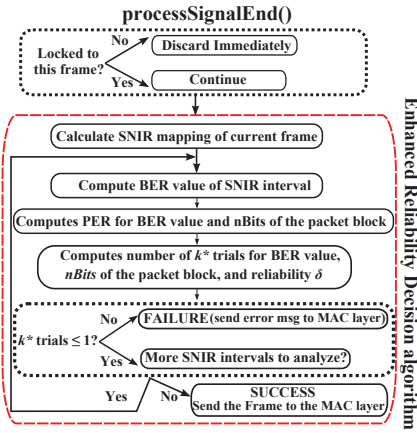


Figure 5: Upgraded “processSignalEnd()” method in MiXiM with Enhanced Reliability Decider.

For the sake of simplicity more details concerning the different methods considered in the source code of the MiXiM framework are described in [16]. The reliability decision algorithm implemented in the MiXiM framework is presented in Figure 5, and is as follows:

1. When a frame is received in the *processNewSignal()* method, the SNIR mapping is determined for the frame that is considered as the desired one;
2. After determining the SNIR mappings corresponding to the different overlapping zones of the desired frame, the value of BER is computed for this specific SNIR interval and with a given block length of  $nBits$ , which in turn calculates the value of PER;
3. Based on the PER value, block length and a certain reliability,  $\delta$ , it computes the number of trials,  $k^*$ , needed

to successfully decode this block of  $nBits$ ;

4. After the algorithm checks whether the required number of trials, for a specific value of the PER, is lower or equal to one (i.e.,  $k^* \leq 1$ ). If so, the algorithm checks if there are more SNIR intervals to be analyzed. Otherwise, the frame is immediately discarded;
5. Finally, the algorithm checks if there is more SNIR intervals to be analyzed. If so, it repeats all the steps described above. Otherwise, the frame is decoded with success and it is sent up to the MAC layer.

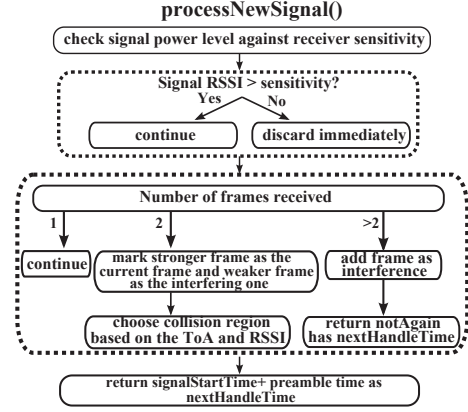


Figure 6: Upgraded “processNewSignal()” method.

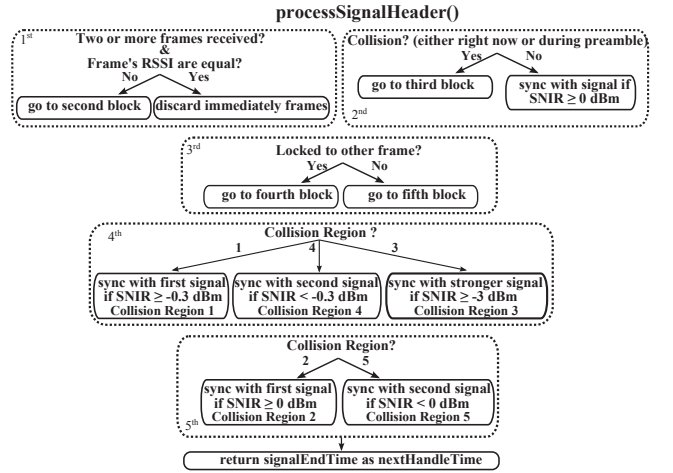


Figure 7: Upgraded “processSignalHeader()” method in MiXiM.

Figures 5, 6 and 7 present a simplified representation of the overall behaviour of the *Decider* with the FC capability. The implementation was added in all the three functions of the *Decider* that process the frame at different points in time, during its reception. These functions are the *processNewSignal()*, *processSignalHeader()* and *processSignalEnd()* ones and are located in the *Decider802154Narrow:processSignal()* module. The description of the enhanced *Decider* with FC capabilities has some parts that have been omitted, because their are the ones that have not been changed. Also, some modifications have been made at the function

`getSignalState()` from the *BaseDecider* module. This function was updated in order to handle two or more frames, so that the remaining ones are not considered as interfering frames anymore.

### 4.3 Frame Capture Decision Thresholds

From all the literature and research works we concluded that, depending on the current state of the receiver as well as the current state of the interference, there can be multiple SNIR capture decision thresholds in which a newly arriving frame must attain in order to enable the receiver to start decoding it.

The thresholds considered for our performance evaluation are based on simulation experiments and the observed behaviour from the works in [4, 12]. In the first set of simulations performed with the FC feature, the considered thresholds were the same as the ones applied to IEEE 802.11a in the work from the authors of [12]. In the second set of simulations, the FC thresholds were based on the behaviour observed from the curves of Figure 3 from the work of [4]. In the second set of simulations the thresholds are lower than the ones from [12]. Then, based on the conducted simulations, it is possible to tune the thresholds in order to guarantee the maximum packet reception possible when considering one interfering frame. These thresholds are defined in Figure 7 and summarized in Table 2. For the scenarios with more than one interfering frame, these thresholds have been maintained. Therefore, it should be kept in mind that these thresholds do not always guarantee the maximum successful packet reception in all the scenarios. Rather, the objective of the FC is to increase the data packet success rate.

**Table 2: SNIR thresholds for simulator.**

| Collision Region | SNIR Threshold [dBm] |
|------------------|----------------------|
| 1                | -0.3                 |
| 2                | 0                    |
| 3                | -3                   |
| 4                | -0.3                 |
| 5                | 0                    |

## 5. PERFORMANCE EVALUATION

In order to test the FC effect and the Enhanced Reliability Decision algorithm we implemented them in the MiXiM framework. To properly evaluate the FC feature with the new decision algorithm, a performance comparison must be performed between the *Decider* with the FC enabled and disabled for the considered collision regions. The FC has certainly a significant effect on the throughput. If a frame is captured, a collision no longer necessarily means loss of capacity. FC always occurs during a collision (i.e., the transceiver is able to capture a frame in favour of a weaker frame). Hence, any scenario where many collisions occur is interesting for analysis. Therefore, all the simulated scenarios induce collisions, to better evaluate the FC effect. The intention is to show by means of simulations that FC has a considerable impact on the performance of networks with broadcast traffic.

### 5.1 Simulation Scenario

In the simulations, the IEEE 802.15.4 outdoor channel model is considered, which considers fast fading and shad-

owing effects. The node topology represents a tight cluster of dense deployed wireless nodes, which is a worst-case situation in terms of collisions. We assume that the sensor nodes have random positioning mobility by means of the random Waypoint mobility algorithm repeated each mobility interval,  $m_{interval}$ . The reason for applying this type of mobility model to the nodes is the need to vary the RSSI from the receiver node. In the MiXiM framework, the RSSI of a frame sent by a node varies depending on the distance to the receiver node. Nodes are deployed using a 2D Poisson process on a  $80 \times 80 m^2$  area (i.e.,  $x, y \in [0, 80] m$ ). The number of contending nodes is kept constant during the simulations, in order to properly evaluate the effective data packet delivery. There is only one sink node while the remaining ones are sources (and send broadcast packets).

For each deployment with  $n$  contending nodes, a set of 6 seeds has been chosen for the random number generator (which has six degrees of freedom). Each simulation takes 100000 seconds of simulation time, corresponding to 19998 attempts of transmitting frames for each seed. The remaining simulation parameters are summarized in Table 3.

**Table 3: Simulation parameters.**

| Description               | Symbol               | Value    |
|---------------------------|----------------------|----------|
| Data rate                 | $R$                  | 250 kb/s |
| Mobility interval         | $m_{interval}$       | 3 s      |
| Simulation time           | $T$                  | 100000 s |
| Packet length             | $L_{data}$           | 50 bytes |
| Maximum number of trials  | $k_{max}^*$          | 1        |
| Thermal Noise             | $N_0$                | -110 dBm |
| Sensitivity               | $S_{min}$            | -94 dBm  |
| Transmission power        | $P_{tx}$             | 1 mW     |
| Frame generation interval | $t_{generate\_data}$ | 5 s      |

In this set of FC simulations, the Texas Instruments CC 2420 low-power radio transceiver is considered. Each time the application layer generates a frame, it only transmits the frame after the node has chosen a new position in the simulation area. Radio switching times have been omitted, i.e., a receiving radio can switch between the sending and receiving mode instantly.

### 5.2 Results for the Default Decider with FC

To compare the default algorithm from the *Decider* with the new Enhanced Reliability Decision algorithm with FC we ran simulations in order to plot the normalized SNIR histogram distributions for the MiXiM *Decider* default implementation under the five collision regions (1 to 5). We observed that the SNIR turning point (to initiate always receiving the packets successfully) differs depending on the Collision Region. The values of the SNIR turning point are summarized in Table 4. We also concluded that there are more packets received with errors than with success. With the default *Decider* implementation, there is a critical zone in which, for the same values of SNIR the packet is received either with no errors or with errors. This critical zone varies depending on the collision region and is summarized in Table 4. In addition, Table 4 presents the SNIR intervals for the packets that are received with success and failure zones.

The existence of the critical zone is due to the random comparison that is performed in the default *Decider* implementation. Apart from the value of the SNIR, the final

Table 4: SNIR distribution for the default MiXiM *Decider* for different collision regions.

| Collision region | SNIR interval for  |                   |                   |
|------------------|--------------------|-------------------|-------------------|
|                  | Critical zone [dB] | Success zone [dB] | Failure zone [dB] |
| 1                | [-2; 0]            | >0                | <-2               |
| 2                | [-2; 0.5]          | >-0.5             | <-2               |
| 3                | -                  | $\geq 0$          | <0                |
| 4                | [-3; 0]            | >0                | <-3               |
| 5                | [-8; 0]            | >0                | <-8               |

decision on successfully decoding the packet depends on the comparison with a random number, which is not so effective.

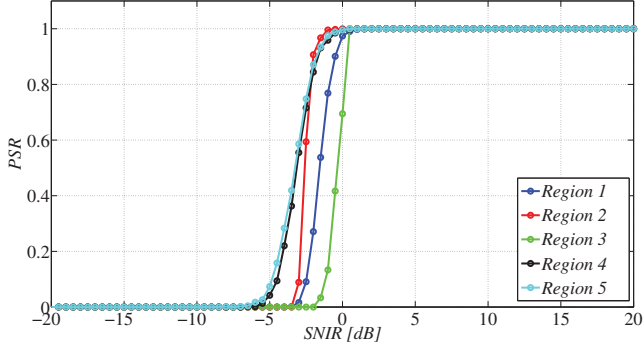


Figure 8: PSR as a function of SNIR for collision regions (1 to 5) of the default *Decider*.

Figure 8 presents the PSR as a function of SNIR was also evaluated with the default *Decider* implementation for the different collision regions. It can be observed in Figure 8 that, in all the collision regions, the PSR achieves the maximum value for SNIRs values higher than about 0 dB. By comparing each of the collision region, one considers that Collision Region 3 (green line) is the one that presents a non-null PSR for a SNIR of around -2 dB. This happens because this region corresponds to the full packet overlapping case. Since there are more bits of the packet being overlapped, the required SNIR to obtain a non-null PSR must be higher than in the other collision regions. The values of the required SNIR to achieve a non-null PSR are summarized in Table 5 for the remaining collision regions.

Table 5: Values of the SNIR for a non-null PSR.

| Collision Region | SNIR [dB]   |
|------------------|-------------|
| 1                | $\geq -4$   |
| 2                | $\geq -4.3$ |
| 3                | $\geq -2$   |
| 4                | $\geq -6$   |
| 5                | $\geq -6$   |

### 5.3 Results for the Enhanced Decider with FC

After implementing the reliability decision algorithm as well as the FC feature in the MiXiM framework, the implementation of the enhanced *Decider* was verified by means of simulations. The intention is to show the advantages of considering a PHY layer with FC capabilities jointly with the Enhanced Reliability Decision algorithm.

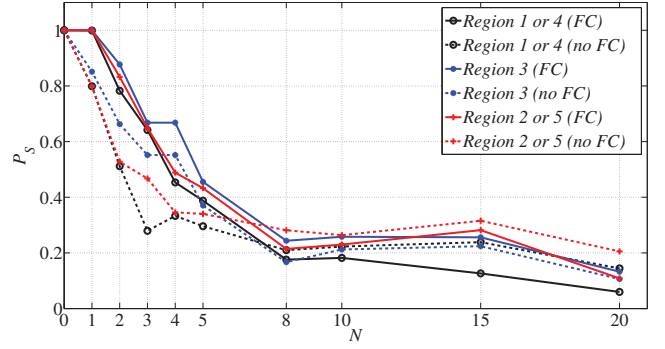


Figure 9: Probability of success,  $P_S$ , as a function of the number of interfering nodes,  $N$ , for  $(\delta_1 = 0.9)$ .

Figure 9 shows the variation of the probability of success,  $P_S$ , within the number of interfering nodes, for each of the collision region when the FC effect is enabled or disabled. A reliability of  $\delta = \delta_1 = 0.9$  is considered. By comparing the curves, one can conclude that for  $N < 8$ , FC leads to higher values of the PSR in all the collision regions. It is also shown that for  $N < 8$  interfering nodes there is no advantage of using FC. The collision regions evaluated in this work, are always the worst possible cases because the interfering frames overlap the desired packet for almost 95 % of the section. All the cases whose overlap is less than the ones studied in this work will present higher values for the PSR when FC is enabled, even for higher number of interfering nodes. The collision region that presents the highest values for the PSR (in average) is the Collision Region 3 (blue lines), while the one that presents the lowest PSR values (in average) are the Collision Regions 1 or 4 (black lines). One can also conclude from Figure 9 that, for all collision regions, the values for the PSR decrease sharply as  $N$  increases up to eight interfering nodes. For a number of interfering nodes higher or equal than eight, the value of the PSR decreases at a slow rate as the interfering nodes increases.

To measure the gains achieved when using a PHY layer with FC enabled the mean absolute error (MAE) for the different collision regions was calculated (for a value of the reliability  $\delta = \delta_1 = 0.9$ ). The highest gain achieved with FC enabled is about 38 % in the Collision Regions 1 or 4. In the Collision Region 3 the highest achieved value for is 21 %, while for the Collision Regions 2 or 5 the highest value is 30 %. All these values for the MAE are compared with the *Decider* in which the FC effect feature is disabled, but the reliability decision algorithm is maintained.

The values presented before are the absolute values of the gain, and may not reflect the negative gains (i.e., loss) that the use of the FC presents when  $N \geq 8$ . The use of the FC effect in Collision Regions 1, 2, 4 and 5,  $N \in \{8, 10\}$ , leads to a negative gain of 5 %, while, for  $N = 20$ , it leads to a negative gain of 10 %. The negative gain means that the employment of the FC effect in a specific situation is not advantageous, which leads to performance losses. Only in the Collision Region 3 there is a positive gain of about 5 %, for  $N \in \{8, 10\}$ , and 3 %, for  $N = 20$ . Table 6 presents a summary of the comparison for the average gains between the cases when FC is enabled and disabled.

In Table 6 there is a distinction between the absolute and the non absolute values. The former are based on the val-

**Table 6: Average gains ( $G_n$ ) between the cases of FC feature enabled and disabled.**

| Collision region | Gain ( $G_n$ ) [%] |              |                      |
|------------------|--------------------|--------------|----------------------|
|                  | Absolute           | Non absolute | Absolute ( $N < 8$ ) |
| 1 and 4          | 13.39              | 9.85         | 17.43                |
| 3                | 9.21               | 9.21         | 11.33                |
| 2 and 5          | 12.46              | 8.06         | 15.39                |

ues of the MAE (in which the gains are always positive). The latter are based on the difference of the probability of success between the cases when the FC is enabled and disabled (in which the gains can be either positive or negative). However, the last column of Table 6 only refers to the average gain for each collision region when  $N < 8$  (in which FC is advantageous). For Collision Region 3 the use FC effect is always advantageous. After evaluating the PSR for different collision regions with and with no FC feature, the influence of the reliability on the probability of success was analyzed. In this analysis, the Collision Region 3 was considered, because it is the region in which the interfering frame completely overlaps the desired signal, becoming the worst possible scenario. All other collision regions, presenting a lower packet overlapping percentage, will result in higher values for the PSR. Figure 10 presents the variation of the probability of success for the Collision Region 3, with the FC effect enabled and disabled, with  $\delta \in \{0.9, 0.99\}$ .

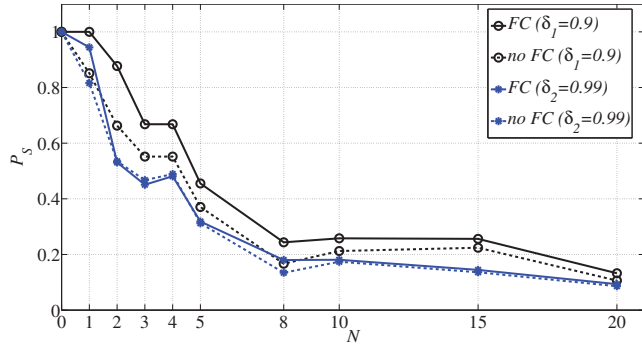


**Figure 10: Probability of success as a function of the number of interfering nodes,  $N$ , for the Collision Region 3, with the FC effect enabled and disabled, with  $\delta_1 = 0.9$  and  $\delta_2 = 0.99$ .**

In Figure 10 the probability of success for a reliability of  $\delta = \delta_1 = 0.9$  is always higher than for  $\delta = \delta_2 = 0.99$  (with and with no FC enabled). This result is expected since, with the increase of the reliability the minimum BER required to accept a packet becomes higher. For  $\delta = \delta_2 = 0.99$  (blue lines), the behaviour is similar to the case of  $\delta = \delta_1 = 0.9$ , as the number of interfering nodes increases. Moreover, for a reliability of  $\delta = \delta_2 = 0.99$  the gains obtained from enabling the FC feature are not so notorious as for  $\delta = \delta_1 = 0.9$ . With  $\delta = \delta_2 = 0.99$  (differently from considering lower values of  $\delta$ ), these values can be interpreted as approximately the lowest (worst case) achievable probability of success when considering a PHY layer with and with no FC.

A higher reliability means less packets received successfully. However, it guarantees that packets with lower BER values are delivered at the MAC layer level.

## 5.4 SCP-MAC Performance Evaluation

In the previous sections, the packet success ratio has been evaluated in different collision regions, with and without enabling the FC feature for a basic MAC protocol without any kind of CS or collision avoidance mechanism. Therefore, simulations were conducted with the FC effect feature enabled/disabled considering the SCP-MAC [18] protocol. For the SCP-MAC, since the nodes are all synchronized, the only possible overlapping region is the Collision Region 3 (interfering frames completely overlap the desired signal).

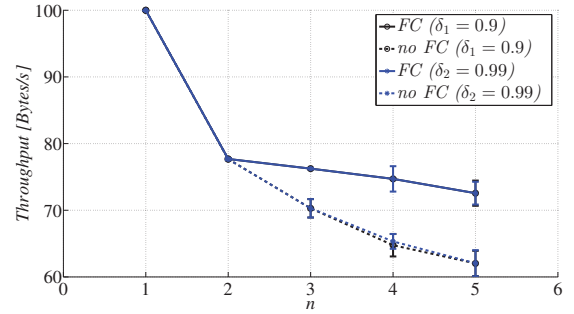


**Figure 11: Throughput of SCP-MAC when FC is enabled and disabled with  $\delta_1 = 0.9$  and  $\delta_2 = 0.99$ .**

Figure 11 presents the throughput obtained for the SCP-MAC protocol as the number of transmitters,  $n$ , in the network increases. These results consider the FC feature enabled and disabled, as well as reliabilities of  $\delta = \delta_1 = 0.9$  and  $\delta = \delta_2 = 0.99$ . Figure 11 shows that, for  $n \geq 2$  when the FC is enabled, the achieved throughput increases up to 10 %, compared with the achieved throughput when the FC is not enabled. By comparing the achieved gains (when FC is enabled) with the gains from Table 6 (for Collision Region 3), we conclude that the values are similar and consistent.

## 6. CONCLUSIONS

This work proposes the Enhanced Reliability Decision algorithm for the IEEE 802.15.4 PHY layer and addresses the implementation of the FC effect feature in the IEEE 802.15.4 compliant PHY layer from the MiXiM framework. The proposed decision algorithm utilizes the SNIR and the length of the packet to guarantee the delivery, to the MAC layer, of a packet received at the PHY layer with a certain reliability.

It has been shown that enabling the FC effect leads to different delivery ratio gains ( $G_n$ ) for each one of the presented regions. Collision regions 1 and 4 attain  $G_n=17.43$  %, collision region 3 achieves values of  $G_n=11.33$  % while collision regions 2 and 5 attain values of  $G_n=15.39$  % for a maximum number of eight interfering nodes. Collision region 3 is considered as the worst case possible (full frame overlapping), in which the FC is always advantageous. The probability of success (in the presence or absence of FC) is always higher for a reliability of  $\delta_1=0.9$  than for  $\delta_2=0.99$ . With the increase of reliability, the minimum BER required to accept a packet is higher than for lower values of the reliability. Results are also presented for the SCP-MAC protocol, while enabling the FC effect for different values of the reliability, in which the only possible overlapping scenario is the collision region 3. These results shown that, for  $n \geq 2$  with the FC effect enabled, the achieved throughput increases

around 10 % when compared to the case where the FC is not enabled. By comparing the gains achieved (when FC is enabled) with the gains presented in Table 6 for the collision region 3, one concludes that the values are similar and consistent. Future work involves the real implementation of the frame capture for newer radio transceivers.

## 7. ACKNOWLEDGMENTS

This work was supported by the PhD FCT (Fundação para a Ciência e Tecnologia) grant SFRH/BD/38356/2007, the programmatic budget from Instituto de Telecomunicações, COST IC0902, COST IC0905 “TERRA”, COST IC1004, OPPORTUNISTIC-CR (PTDC/EEA-TEL/115981/2009), PROENERGY-WSN (PTDC/EEA-TEL/122681/2010), PEst-OE/EEI/LA0008/2013, CREaTION (EXCL/EEI-TEL/0067/2012) and by PLANOPTI (FP7-PEOPLE-2009-RG) and a special thanks to Professor Pedro Sebastião.

## 8. REFERENCES

- [1] IEEE Standard for Information technology - Telecommunications and information exchange between systems - Local and metropolitan area networks- Specific requirements Part 15.4: Wireless Medium Access Control (MAC) and Physical Layer (PHY) Specifications for Low-Rate Wireless Personal Area Networks (WPANs) . Technical report, 2006.
- [2] Chipcon CC2420 Datasheet: <http://focus.ti.com/lit/ds/symlink/cc2420.pdf>, Texas Instruments, 2007.
- [3] H. Chang, V. Misra, and D. Rubenstein. A General Model and Analysis of Physical Layer Capture in 802.11 Networks. In *Proc. of Annual Joint Conference of the IEEE Computer and Communications Societies (IEEE Infocom)*, Barcelona, Spain, April 2006.
- [4] B. Firner, C. Xu, R. Howard, and Y. Zhang. Multiple receiver strategies for minimizing packet loss in dense sensor networks. In *Proc. of the eleventh ACM international symposium on Mobile ad hoc networking and computing (MobiHoc'10)*, pages 211–220, Chicago, Illinois, USA, September 2010.
- [5] C. Gezer, C. Buratti, and R. Verdone. Capture effect in IEEE 802.15.4 networks: modelling and experimentation. In *Proc. of the 5th IEEE international conference on Wireless pervasive computing (ISWPC'10)*, pages 204–209, Mondena, Italy, May 2010.
- [6] I. Guvenc, S. Gezici, Z. Sahinoglu, and U. C. Kozat. *Reliable Communications for Short-Range Wireless Systems*. Cambridge University Press, United Kingdom, 2011.
- [7] H. Karl and A. Willig. *Protocols and Architectures for Wireless Sensor Networks*. John Wiley & Sons, 2005.
- [8] A. Kochut, A. Vasan, A. Shankar, and A. Agrawala. Sniffing Out the Correct Physical Layer Capture Model in 802.11b. In *Proc. of the 12th IEEE International Conference on Network Protocols (ICNP 2004)*, pages 252–261, Berlin, Germany, October 2004.
- [9] A. Köpke, M. Swigulski, K. Wessel, D. Willkomm, P. T. K. Haneveld, T. E. V. Parker, O. W. Visser, H. S. Lichte, and S. Valentin. Simulating wireless and mobile networks in OMNeT++ the MiXiM vision. In *Proc. of the 1st international conference on Simulation tools and techniques for communications, networks and systems & workshops (Simutools '08)*, pages 71–79, Marseille, France, March 2008.
- [10] M. Lacage and T. R. Henderson. Yet another network simulator. In *Proc. of the 2006 workshop on ns-2: the IP network simulator (WNS2 '06)*, Pisa, Italy, October 2006.
- [11] J. Lee, W. Kim, S. J. Lee, D. Jo, J. Ryu, T. Kwon, and Y. Choi. An experimental study on the capture effect in 802.11a networks. In *Proc. of the second ACM international workshop on Wireless network testbeds, experimental evaluation and characterization (WinTECH'07)*, pages 19–26, New York, NY, USA, 2007. ACM.
- [12] J. Lee, J. Ryu, S. Lee, and T. Kwon. Revamping the IEEE 802.11a PHY simulation models. In *Proc. of the 11th international symposium on Modeling, analysis and simulation of wireless and mobile systems (MSWiM'08)*, pages 28–36, Vancouver, British Columbia, Canada, 2008.
- [13] N. B. Priyantha, A. Chakraborty, and H. Balakrishnan. The Cricket location-support system. In *Proc. of the 6th annual international conference on Mobile computing and networking (MobiCom'00)*, pages 32–43, Boston, Massachusetts, USA, August 2000.
- [14] G. F. Riley and T. R. Henderson. The ns-3 Network Simulator Modeling and Tools for Network Simulation. In K. Wehrle, M. Güneş, and J. Gross, editors, *Modeling and Tools for Network Simulation*, chapter 2, pages 15–34. Springer Verlag, Berlin, Heidelberg, 2010.
- [15] A. Varga. Omnet++. In K. Wehrle, M. Güneş, and J. Gross, editors, *Modeling and Tools for Network Simulation*, pages 35–58. Springer Verlag, September 2010.
- [16] K. Wessel, M. Swigulski, A. Köpke, and D. Willkomm. MiXiM: the physical layer an architecture overview. In *Proc. of the 2nd International Conference on Simulation Tools and Techniques (Simutools'09)*, pages 78–86, Rome, Italy, March 2009.
- [17] K. Whitehouse, A. Woo, F. Jiang, J. Polastre, and D. Culler. Exploiting the capture effect for collision detection and recovery. In *Proc. of the 2nd IEEE workshop on Embedded Networked Sensors (EmNetS-II)*, pages 45–52, Washington, DC, USA, May 2005.
- [18] W. Ye, F. Silva, and J. Heidemann. Ultra-Low Duty Cycle MAC with Scheduled Channel Polling. In *Proc. of the Fourth ACM International Conference on Embedded Networked Sensor Systems (SenSys'06)*, pages 321–333, Boulder, Colorado, USA, November 2006.